

Scaled Brownian motion with renewal resetting

Anna S. Bodrova,¹ Aleksei V. Chechkin,^{2,3} and Igor M. Sokolov¹

¹*Humboldt University, Department of Physics, Newtonstrasse 15, 12489 Berlin, Germany*

²*Institute of Physics and Astronomy, University of Potsdam, 14476 Potsdam, Germany*

³*Akhiezer Institute for Theoretical Physics, Kharkov Institute of Physics and Technology, Kharkov 61108, Ukraine*

Parallel to our previous work [1] we investigate an intermittent stochastic process in which the diffusive motion with time-dependent diffusion coefficient $D(t) \sim t^{\alpha-1}$ with $\alpha > 0$ (scaled Brownian motion, SBM) is stochastically reset to its initial position and starts anew. At variance with our previous work, where the resetting process did not affect the diffusion coefficient's time dependence, in the present work we discuss the fully renewal situation, in which the memory on the value of the diffusion coefficient at a resetting time is erased so that the whole process is a renewal one. We show that the properties of such process are vastly different from the ones of the process discussed in our previous work, and stress the importance of partial memory erasing / retaining in processes under resetting. In addition we discuss the first passage properties of the SBM with renewal resetting and consider the dependence of the efficiency of search on the parameters of the process.

I. INTRODUCTION

This work is a continuation of our previous one [1], where we considered a random process arising from the resetting of a scaled Brownian motion (SBM) to its initial position, which resetting, however, did not affect the explicit time-dependence of its diffusion coefficient. This corresponds to the retaining of the memory on the instant of time when the SBM started. To see how important this memory is, we have to compare the results for this case with the ones for the case when the memory is erased, and the SBM process starts anew, that is, when all motions within the epochs between two subsequent resetting events can be considered as statistical copies of each other, so that the whole process is a renewal one.

There are several reasons to discuss this problem of the fully renewal SBM in a separate publication. First, the situation at hand is much simpler, and a larger program of investigations may be performed. Notably, the renewal nature of the process allows for a very simple discussion of its first passage properties [2], a problem which was not considered in the non-renewal case. Second, the renewal situations are the ones typically considered in other processes, so that the results can be immediately compared to such.

The overview of previous works on resetting processes is given in [1] and will not be repeated here. A short introduction to the first passage properties is however due, and is given below.

The interest to the first passage properties of stochastic processes under resetting was motivated by the problems of optimal search [3]. Since searching for a target at an unknown location may go in a completely wrong direction, it might be useful to return to the initial point, and to start from the very beginning. This behavior can be modeled by a stochastic exploration process, which is interrupted by random resettings to the initial position. Examples of such processes are found in many fields such as computer science [4], biochemistry [5] and biology [6]. In computer science random walks with stochastic restarts represent a useful strategy to optimize search algorithms in hard computational problems [4]. In biochemistry, resetting, connected with a departure of an enzyme from a substrate, may increase the rate of product formation [5]. In biology, gene transcription by RNA polymerases can be viewed as a diffusion process with stochastic resetting [6]. The movements of foraging animals usually involve a local search for food, interrupted by long-range moves during which they relocate to a different territory, where the search starts anew [3].

One of the main characteristics of the efficiency of a search process is the mean first passage time (MFPT) - the time, at which the particle hits the target for the first time on the average [7, 8]. Early work concentrated on a searcher performing one-dimensional Brownian motion with Poissonian resetting [9–11]. While the MFPT to a target for a diffusing particle in absence of resetting diverges, in presence of resetting it turns finite, and there exist an optimal rate of resetting which minimizes the MFPT. The discussion has been extended to two and higher dimensions in [12, 13]. While for ordinary Brownian motion the optimal resetting rate depends only on the distance x_0 between the target and the origin, and on the diffusion coefficient D of the particle, in the case of active particles it may depend on finer details of motion not comprized in the effective diffusion coefficient [14]. Another search process is the one in which an individual searcher has a random, finite lifetime, and, when it expires, is replaced by a new one starting at the origin [15]. Refs. [16, 17] discuss the MFPT for the case of Lévy flights with discrete time and Poissonian resetting processes, and discuss the parameter values minizing the MFPT for several cases including random distribution of targets. Other types of the waiting time distributions for resetting events have been studies in [18–21]. It has been shown that the resetting at a constant pace is the most effective strategy [2, 13, 18, 21]. Ordinary Brownian motion with power law waiting time densities for resetting events has been investigated in [22]. It has been shown that there

exist a certain power-law exponent minimizing the MFPT for a given target position.

In the present work we investigate particles performing scaled Brownian motion (SBM) [23–25], a stochastic process with time-dependent diffusion coefficient, between the resetting events. We calculate the mean-squared displacement (MSD), the probability density function (PDF) of this process and the MFPT to a given target. In our previous paper [1] we have considered the non-renewal process when the diffusion coefficient remains unaffected by the resetting events. In the present work we concentrate on the renewal situation, where the diffusion coefficient is also reset, and the displacement process is rejuvenated under resetting so that the whole process is a renewal one. For this process a larger program of investigation than in [1] can be performed. The plan of the paper is as follows. In the next Section II we give a brief overview of the properties of SBM. In Section III we introduce the general analytic expressions for MSD and PDF and describe the algorithm of numerical simulations. In Section IV we calculate MSD and PDF for Poissonian resetting, and in Section V - the first passage time. In Sections VI and VII we discuss power-law resetting for $0 < \beta < 1$ and $\beta > 1$, correspondingly, and in Section VIII derive first-passage time for power-law resetting. We give our conclusions in Section IX.

II. SCALED BROWNIAN MOTION

Scaled Brownian motion [23] is the diffusion process with explicitly time-dependent diffusion coefficient $D(t) \sim t^{\alpha-1}$, in which the mean squared displacement grows as

$$\langle x^2(t) \rangle = 2K_\alpha t^\alpha \quad (1)$$

with K_α being the generalized diffusion coefficient. For $\alpha = 1$ the process is identical to normal, Fickian diffusion, for $\alpha > 1$ it is super- and for $0 < \alpha < 1$ subdiffusive. We define SBM in terms of the stochastic process

$$\frac{dx(t)}{dt} = \sqrt{2D(t)}\eta(t) \quad (2)$$

with Gaussian noise $\eta(t)$ possessing zero mean $\langle \eta(t) \rangle = 0$ and the correlation function

$$\langle \eta(t_1)\eta(t_2) \rangle = \delta(t_1 - t_2), \quad (3)$$

and with

$$D(t) = \alpha K_\alpha t^{\alpha-1}. \quad (4)$$

The probability density function (PDF) of displacements of particles performing free SBM starting at time t' is Gaussian,

$$p_0(x, t - t') = \frac{1}{\sqrt{4\pi K_\alpha (t - t')^\alpha}} \exp\left(-\frac{x^2}{4K_\alpha (t - t')^\alpha}\right). \quad (5)$$

III. PDF, MSD, AND MFPT FOR SCALED BROWNIAN MOTION WITH RENEWAL RESETTING

Let us assume that the particle starts its motion at the origin and returns there at the resetting events. Then, for a renewal (rejuvenating) case, the probability to find the particle at location x at time t reads

$$p(x, t) = \Psi(t)p_0(x, t) + \int_0^t dt' \kappa(t')\Psi(t - t')p_0(x, t - t'), \quad (6)$$

where $\kappa(t)$ is the rate of resetting events (in general time-dependent), and $\Psi(t)$ is the propability that no resetting events took place before time t (the survival probability). Both can be expressed through the waiting time density $\psi(t)$ for the renewal events, see [1]. Here the first term in the right-hand side corresponds to trajectories in which there are no resets at all, and the second one accounts for the cases where the last reset took place at time t' . The only difference with the case considered in [1] is that the function $p_0(x, t, t')$ now only depends on the difference of its two temporal arguments, c.f. Eqs.(10) and (12) of [1]. At long times $t \rightarrow \infty$ the first term may be safely neglected and the PDF is given only by the second term in Eq. (6):

$$p(x, t) \simeq \int_0^t dt' \kappa(t')\Psi(t - t')p_0(x, t - t'). \quad (7)$$

Multiplying Eq. (6) by x^2 and performing the integration with respect to x , we get the equation for the MSD of particles

$$\langle x^2(t) \rangle = 2K_\alpha t^\alpha \Psi(t) + 2K_\alpha \int_0^t dt' \kappa(t') \Psi(t-t') (t-t')^\alpha. \quad (8)$$

At long times $t \rightarrow \infty$ the first term may be neglected, and we obtain for the MSD

$$\langle x^2(t) \rangle \simeq 2K_\alpha \int_0^t dt' \kappa(t') \Psi(t-t') (t-t')^\alpha. \quad (9)$$

Below we will investigate the behavior of the PDF, Eq.(6) and of the MSD, Eq.(8) for exponential and power-law waiting time PDFs in the resetting process. Moreover, we will study the first passage properties of the corresponding processes to some point x_0 on a line.

Note that the PDF and the MSD of the process depend only on the Gaussian property of the displacement process at a single time, and therefore will be the same for all (Markovian or non-Markovian) Gaussian processes with the same $\langle x^2(t) \rangle$ in free motion, e.g. for the fractional Brownian motion [26], provided resetting erases memory of the displacement process, and the particle's displacements between the two subsequent resetting events can be considered as statistical copies of each other.

To investigate the first passage time we use the approach put forward in [2]. There, using the renewal property of the whole process, one derives the expression for the first hitting time which in the case of a single target we consider here reads:

$$\begin{aligned} p(t) = & \Psi(t)\phi(t) + \int_0^t \psi(t')\Phi(t')\Psi(t-t')\phi(t-t')dt' \\ & + \int_0^t dt' \psi(t')\Phi(t') \int_0^{t-t'} dt'' \psi(t'')\Phi(t'')\Psi(t-t'-t'')\phi(t-t'-t'') + \dots, \end{aligned} \quad (10)$$

where the first term is the probability density of hitting the target in the first successful run which was not reset until the hitting time, the second term describes the situation in which the first run was not successful and was terminated by resetting at time t' , while the second run is successful, etc. Here $\phi(t)dt$ is the probability that the target is hit in the time interval between t and $t+dt$, and was never hit before, and $\Phi(t) = 1 - \int_0^t \phi(t')dt'$ is the survival probability of a target in a single run. The cumulative distribution function for hitting in an uninterrupted run will be denoted by $F(t) = \int_0^t \phi(t')dt'$. Denoting $K(t) = \Psi(t)\phi(t)$ and $R(t) = \psi(t)\Phi(t)$, and turning to the Laplace domain, we get

$$\tilde{p}(s) = \frac{\tilde{K}(s)}{1 - \tilde{R}(s)} \quad (11)$$

with $\tilde{K}_i(s)$ being the Laplace transform of $K(t)$, and $\tilde{R}(s)$ is the Laplace transform of $R(t)$. The Laplace transform $\tilde{P}(s)$ of the survival probability $P(t) = 1 - \int_0^t p(t')dt'$ under resetting is then given by

$$\tilde{P}(s) = \frac{1}{s} - \frac{1}{s} \frac{\tilde{K}(s)}{1 - \tilde{R}(s)} = \frac{\tilde{X}(s)}{1 - \tilde{R}(s)} \quad (12)$$

with $\tilde{X}(s) = s^{-1}[1 - \tilde{R}(s) - \tilde{K}(s)]$. The mean first passage time $\tau = \int_0^\infty P(t)dt$ under resetting follows then in form [2]

$$\tau = \frac{X_0}{1 - R_0} \quad (13)$$

with

$$X_0 = \tilde{X}(0) = \int_0^\infty dt \Phi(t) \Psi(t) \quad (14)$$

and

$$R_0 = \tilde{R}(0) = \int_0^\infty dt \Phi(t) \psi(t). \quad (15)$$

The analytical results are compared with numerical simulations.

In the renewal resetting the whole process starts anew at the resetting event, and the memory on its previous course is erased. Therefore the simulation of the process up to the last resetting event is not necessary to get the MSD and the PDF of the particle's positions. The event-driven simulations for MSD and for PDF are performed as follows. For a given sequence of the output times t we simulate the sequence of resetting events, find the time of the last resetting event $t' < t$ and set $x(t') = 0$. Then the position of the particle at time t is distributed according to a Gaussian with zero mean and variance $\langle x^2(t) \rangle = 2K_\alpha(t-t')^\alpha$. The corresponding Gaussian can be obtained from a standard normal distribution generated using the Box-Muller transform. The results are averaged over $N = 10^4$ to 10^6 independent runs.

In order to calculate the first passage time we apply the direct simulation. The time axis is discretized with the step $dt = t_{i+1} - t_i$, and the time of the first resetting T_1 is generated according to the waiting time density $\psi(t)$. Then the particle's motion is simulated, and, if the target was not hit up to T_n , the coordinate is reset to $x = 0$, a new resetting time T_2 is generated, and the simulation repeated, etc. The particle's motion between the resetting events is modelled by a finite-difference analogue of the Langevin equation

$$x_{i+1} = x_i + \xi_i \sqrt{2\alpha K_\alpha (t_i - T_n)^{\alpha-1} dt} \quad (16)$$

(for $T_{n+1} < t_i < T_n$). Here $x_i = x(t_i)$ is the coordinate of the particle at the time t_i , and ξ_i is the random number distributed according to a standard normal distribution generated using the Box-Muller transform. The simulation stops when the particle's coordinate exceeds x_0 for the first time. The first hitting time is then averaged over $N = 10^4$ to 10^5 realizations. The value of αK_α is set to unity in all our simulations. In simulations corresponding to power-law waiting time distributions we set $\tau_0 = 1$.

IV. MSD AND MFPT FOR POISSONIAN RESETTING

The simplest and most studied case corresponds to exponentially distributed waiting times between resets

$$\psi(t) = r e^{-rt}. \quad (17)$$

The survival probability is given by

$$\Psi(t) = 1 - \int_0^t \psi(t') dt' = e^{-rt}. \quad (18)$$

The case of exponential waiting time distribution corresponds to the resetting events constituting a Poisson process on the line characterized by a constant rate, or intensity, r , so that

$$\kappa(t) = r, \quad (19)$$

and does not depend on time.

1. Mean squared displacement

The MSD for SBM with exponential resetting can be obtained by inserting Eqs. (18) and (19) into Eq. (8), and reads

$$\langle x^2(t) \rangle = 2K_\alpha t^\alpha e^{-rt} + \frac{2K_\alpha}{r^\alpha} \gamma(\alpha + 1, rt) \quad (20)$$

with $\gamma(a, z)$ being the lower incomplete Gamma-function

$$\gamma(a, z) = \int_0^z dx e^{-x} x^{a-1}. \quad (21)$$

Expanding the incomplete Gamma-function for $z \rightarrow \infty$

$$\gamma(a, z) \simeq \Gamma(a) - z^{a-1} e^{-z} - \frac{a-1}{z} z^{a-1} e^{-z}, \quad (22)$$

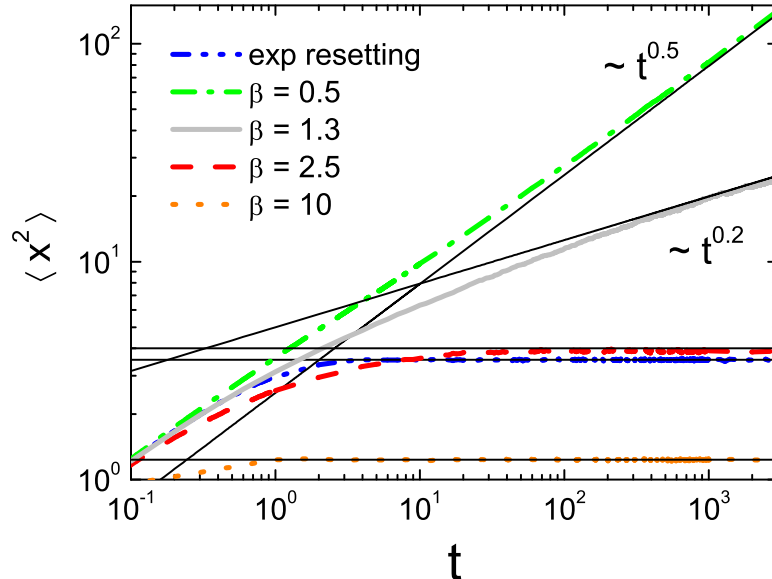


FIG. 1: Mean-squared displacement for power-law and Poissonian resetting with $r = 1$ for $\alpha = 0.5$ as obtained in $N = 10^4$ realizations. Results of simulation are shown by thick colored lines and the analytical asymptotics by thin black solid lines (Eq. (24) for exponential resetting, Eq. (50) for power-law resetting with $0 < \beta < 1$, Eq. (75) for $1 < \beta < 1 + \alpha$, Eq. (77) for $\beta > \alpha + 1$).

we obtain for the MSD

$$\langle x^2(t) \rangle \simeq \frac{2K_\alpha}{r^\alpha} \left[\Gamma(\alpha + 1) - \alpha (rt)^{\alpha-1} e^{-rt} \right]. \quad (23)$$

In the long time limit $t \rightarrow \infty$ the MSD stagnates:

$$\langle x^2(t) \rangle = \frac{2K_\alpha}{r^\alpha} \Gamma(\alpha + 1). \quad (24)$$

In Fig. 1 we show this result together with the results of direct numerical simulation (blue line), and get an excellent agreement.

This behavior of MSD already differs from the result obtained for SBM with a non-rejuvenating diffusion coefficient [1], where the MSD for all $\alpha \neq 1$ shows an explicit time dependence $\langle x^2(t) \rangle \sim t^{\alpha-1}$, and this explicit time dependence of $\langle x^2(t) \rangle$ was a signature of the absence of the stationary state for all kinds of SBM except for the ordinary Brownian case.

For $\alpha = 1$ we recall the ordinary Brownian motion between the resetting events and get at long times the stationary value of MSD

$$\langle x^2(t) \rangle = \frac{2K_1}{r}. \quad (25)$$

2. Probability density function

The probability density function for Poissonian resetting may be obtained by inserting Eqs. (5), (18) and (19) into Eq. (7) which for long times yields

$$p(x, t) \simeq r \int_0^t dt' e^{-r(t-t')} \frac{1}{\sqrt{4\pi K_\alpha (t-t')^\alpha}} \exp\left(-\frac{x^2}{4K_\alpha (t-t')^\alpha}\right). \quad (26)$$

Introducing a new variable $\tau = t - t'$ we rewrite the integral as

$$p(x, t) \simeq \frac{r}{\sqrt{4\pi K_\alpha}} \int_0^t d\tau \exp(-\varphi(\tau)) \tau^{-\frac{\alpha}{2}} \quad (27)$$

with the function $\varphi(\tau) = r\tau + \frac{x^2}{4K_\alpha\tau^\alpha}$ which attains a simple quadratic minimum at

$$\tau_{\min} = \left(\frac{\alpha x^2}{4K_\alpha r} \right)^{\frac{1}{\alpha+1}}. \quad (28)$$

For $0 \ll \tau_{\min} \ll t$ the standard Laplace method can be used:

$$p(x, t) \simeq \frac{r}{\sqrt{4\pi K_\alpha \tau_{\min}^\alpha}} \exp(-\varphi(\tau_{\min})) \int_{-\infty}^{\infty} \exp\left(-\frac{1}{2}\varphi''(\tau_{\min})(\tau - \tau_{\min})^2\right) d\tau, \quad (29)$$

provided $\varphi''(\tau_{\min})$ is large enough. Both conditions correspond to the intermediate asymptotic behavior in x . The final result for this case corresponds to a stationary state and reads:

$$p(x) \simeq \frac{r\sqrt{2}}{\sqrt{\alpha(\alpha+1)}} \left(\frac{\alpha}{4K_\alpha r} \right)^{\frac{1}{\alpha+1}} |x|^{\frac{1-\alpha}{\alpha+1}} \exp\left(-\left(\frac{x^2 r^\alpha}{4K_\alpha}\right)^{\frac{1}{\alpha+1}} \left(\alpha^{\frac{1}{\alpha+1}} + \alpha^{-\frac{\alpha}{\alpha+1}}\right)\right). \quad (30)$$

Fig. 2 presents the results of numerical simulation for $\alpha = 0.5$. The theoretical curve (thin black line) corresponds to the exponential term of Eq.(30) with the preexponential factor replaced by the actual value of $p(x)$ for $x = 0$ calculated from Eq.(26). Contrary to the case of the non-renewal SBM with resetting [1], now the PDF attains a steady, time-independent form in its bulk.

For $\alpha = 1$, the PDF behaves as that for ordinary Brownian motion with exponential resetting, namely, is a two-sided exponential (Laplace) distribution as obtained in [9, 10]:

$$p(x) = \frac{1}{2} \sqrt{\frac{r}{K_1}} \exp\left(-\sqrt{\frac{r}{K_1}} |x|\right). \quad (31)$$

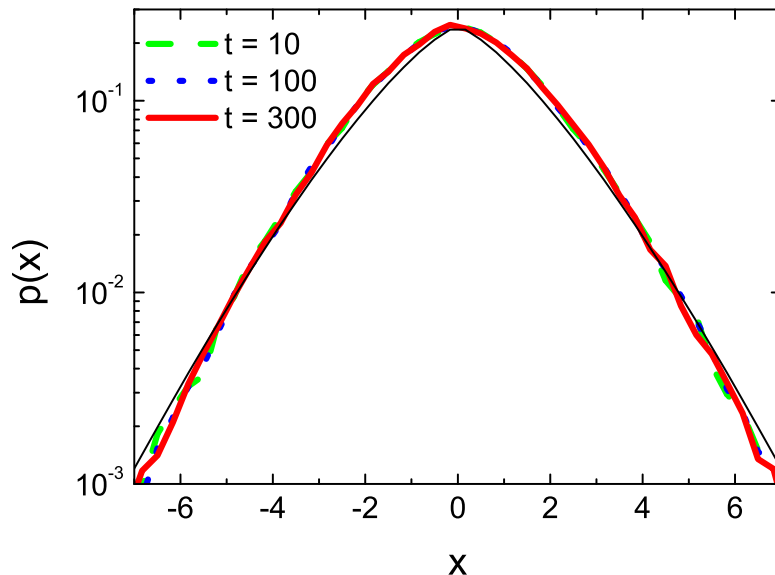


FIG. 2: PDF for SBM with $\alpha = 0.5$ and with Poissonian resetting at different time $t = 10, 100, 300$ (green, blue and red, lines, correspondingly) showing the convergence to a steady state. The theoretical prediction is shown by the thin black solid line, see text for details. Parameters: $N = 10^5$, $r = 1$.

V. MFPT FOR POISSONIAN RESETTING

Now let us calculate the mean time needed for the particle which starts at $x = 0$ to hit a target at position $x_0 \neq 0$. The hitting time probability in a single run of the SBM is given by a change of variables in the Lévy-Smirnov

distribution and reads

$$\phi(t) = \frac{\alpha x_0}{\sqrt{4\pi K_\alpha}} \exp\left(-\frac{x_0^2}{4K_\alpha t^\alpha}\right) t^{-1-\frac{\alpha}{2}}. \quad (32)$$

The survival probability of a target in a single run may be obtained via the integration of the hitting time probability over t

$$\Phi(t) = 1 - \int_0^t \phi(t') dt' = \operatorname{erf}\left(\frac{x_0}{2\sqrt{K_\alpha t^\alpha}}\right). \quad (33)$$

Taking into account that for exponential resetting $\psi(t) = r\Psi(t)$ as given by Eqs. (17) and (18), one gets $R_0 = rX_0$, and the MFPT as given by Eq.(13) can be represented as

$$\tau = \frac{X_0}{1 - rX_0}. \quad (34)$$

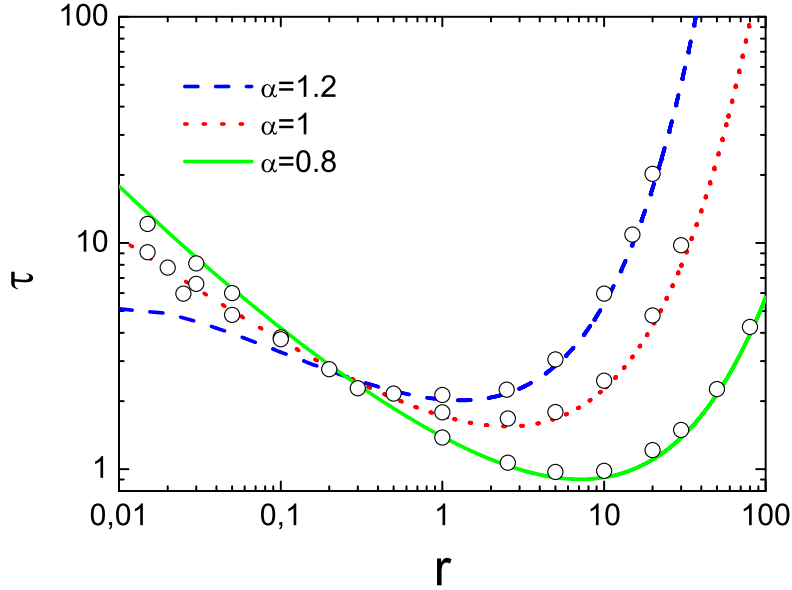


FIG. 3: The mean first passage time τ versus the resetting rate r for different α values. The target position $x_0 = 1$. Analytical results (Eq. 39) are represented by the solid lines, numerical results by dots. An excellent agreement between analytical and numerical results is observed.

The expression for X_0 follows by inserting Eq. (17), Eq. (18) and Eq. (33) into Eq. (14):

$$X_0 = \frac{2}{\sqrt{\pi}} \int_0^\infty dt e^{-rt} \int_0^{\frac{x_0}{2\sqrt{K_\alpha t^\alpha}}} da e^{-a^2}. \quad (35)$$

This expression can be rewritten by changing the order of integrations

$$X_0 = \frac{2}{\sqrt{\pi}} \int_0^\infty da e^{-a^2} \int_0^{\left(\frac{x_0^2}{4K_\alpha a^2}\right)^{1/\alpha}} e^{-rt} dt, \quad (36)$$

after which the inner integral can be evaluated explicitly:

$$X_0 = \frac{1}{r} - \frac{2}{r\sqrt{\pi}} \int_0^\infty da \exp\left(-a^2 - r\left(\frac{x_0^2}{4K_\alpha a^2}\right)^{\frac{1}{\alpha}}\right). \quad (37)$$

The integral can be estimated by using the Laplace method which leads to

$$X_0 \simeq \frac{1}{r} \left(1 - \sqrt{\frac{2\alpha}{\alpha+1}} \exp \left(- \left(\alpha^{\frac{1}{1+\alpha}} + \alpha^{-\frac{\alpha}{1+\alpha}} \right) r^{\frac{\alpha}{\alpha+1}} \left(\frac{x_0^2}{4K_\alpha} \right)^{\frac{1}{\alpha+1}} \right) \right). \quad (38)$$

Inserting this into Eq. (34) we arrive at the final expression for mean first passage time

$$\tau \simeq \frac{1}{r} \left\{ \sqrt{\frac{\alpha+1}{2\alpha}} \exp \left[r^{\frac{\alpha}{\alpha+1}} \left(\frac{x_0^2}{4K_\alpha} \right)^{\frac{1}{\alpha+1}} \left(\alpha^{\frac{1}{1+\alpha}} + \alpha^{-\frac{\alpha}{1+\alpha}} \right) \right] - 1 \right\}. \quad (39)$$

For ordinary Brownian diffusion ($\alpha = 1$) we get the known expression [9], which is now exact:

$$\tau = \frac{1}{r} \left[\exp \left(|x_0| \sqrt{r/K_\alpha} \right) - 1 \right]. \quad (40)$$

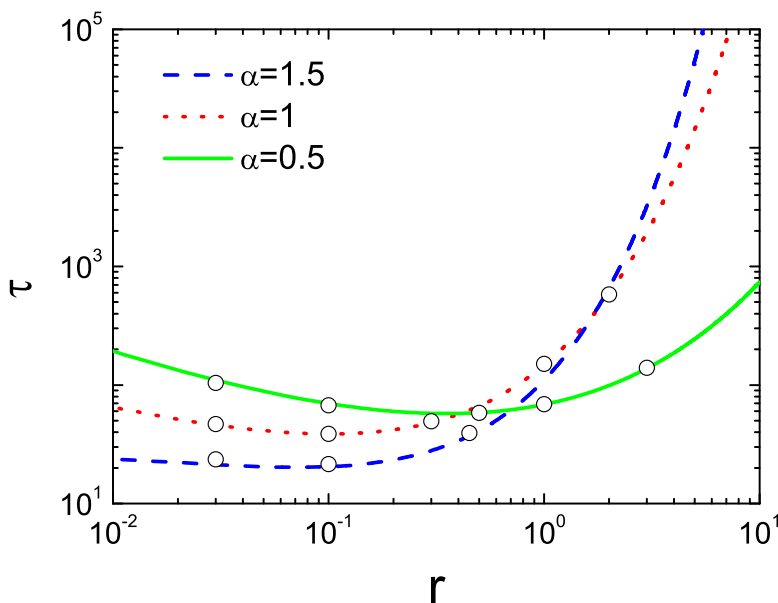


FIG. 4: The mean first passage time τ versus the resetting rate r for different α values. The target position $x_0 = 5$. Results of simulations are shown by the points and the analytical results are represented by the solid lines according to Eq. (39).

The MFPT given by Eq. (39) for different parameter values is shown at Figs. 3 and 4. At very low rates $r \rightarrow 0$ corresponding to free scaled Brownian motion without resetting the MFPT tends to infinity. At $r \rightarrow \infty$ the MFPT also tends to infinity, because the particle does not have enough time to locate the target between the resetting events. Therefore there exists an optimal rate r^* which minimizes the MFPT. Let us first consider the situation where the target is located relatively close to the initial position of the particle ($x_0 = 1$), Fig. 3. In this case the superdiffusive search process is more effective (i.e. leads to shorter MFPT) at relatively small rates $r \leq 0.2$, while at larger rates the target will be found faster under subdiffusive motion. If the distance between the target and initial position of particle increases ($x_0 = 5$), the superdiffusion becomes more favorable for a wider range of r (Fig. 4). This resembles search processes with Lévy flights where large jumps are preferable when the target is located far from the initial position and smaller jumps are preferable when the target is closer to the origin [27].

Minimizing τ (Eq. 39) with respect to r we get the equation for the optimal resetting rate r^*

$$1 - \sqrt{\frac{2\alpha}{\alpha+1}} \exp(-Br^{*c}) = Bcr^{*c} \quad (41)$$

with

$$c = \frac{\alpha}{\alpha+1} \quad (42)$$

and

$$B = \left(\frac{x_0^2}{4K_\alpha} \right)^{\frac{1}{\alpha+1}} \left(\alpha^{\frac{1}{1+\alpha}} + \alpha^{-\frac{\alpha}{1+\alpha}} \right), \quad (43)$$

which can be solved numerically. Fig. 5 shows that the optimal resetting rate r^* decreases with increase of both the distance x_0 between target and initial position (left panel) and α (right panel). The monotonous decrease of r^* as a function x_0 parallels to the case of Lévy flights [16] but does not show the discontinuity observed in this last case.

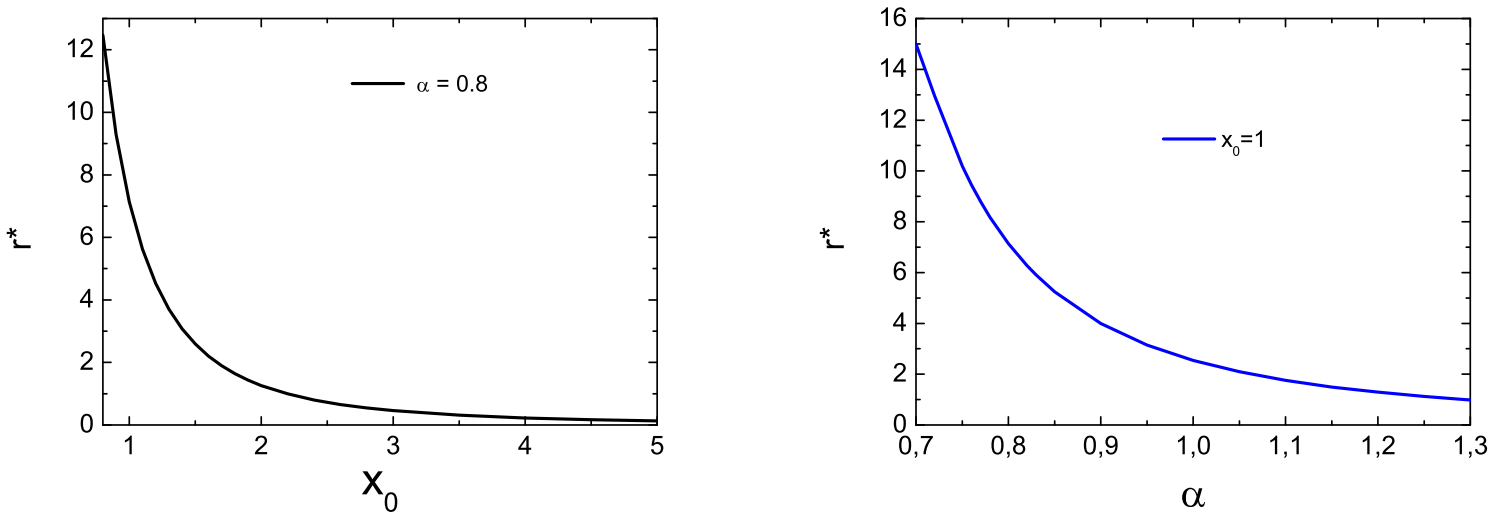


FIG. 5: The optimal resetting rate r^* (obtained as a numerical solution of Eq. (41)) versus the target position x_0 for $\alpha = 0.8$ (left panel) and versus α for $x_0 = 1$ (right panel).

VI. MSD AND PDF WITH POWER-LAW RESETTING, $0 < \beta < 1$

Let us consider the case when the time between successive resets is distributed according to the power law

$$\psi(t) = \frac{\beta/\tau_0}{(1+t/\tau_0)^{1+\beta}}. \quad (44)$$

Here τ_0 is assumed to be constant. The survival probability reads

$$\Psi(t) = (1+t/\tau_0)^{-\beta}. \quad (45)$$

The rate of resetting events is explicitly time-dependent [1]:

$$\kappa(t) = \frac{t^{\beta-1}\tau_0^{-\beta}}{\Gamma(\beta)\Gamma(1-\beta)}. \quad (46)$$

1. Mean squared displacement

Substituting Eqs. (45) and (46) into Eq. (9) we obtain

$$\langle x^2(t) \rangle = \frac{2K_\alpha\tau_0^{-\beta}}{\Gamma(\beta)\Gamma(1-\beta)} \int_0^t dt' t'^{\beta-1} (t-t')^\alpha \left(1 + \frac{t-t'}{\tau_0}\right)^{-\beta}. \quad (47)$$

Assuming $t \gg \tau_0$ we can neglect unity in the last bracket. Changing to a new integration variable $\tau = t'/t$ we get

$$\langle x^2(t) \rangle = \frac{2K_\alpha}{\Gamma(\beta)\Gamma(1-\beta)} t^\alpha \int_0^1 d\tau \tau^{\beta-1} (1-\tau)^{\alpha-\beta}, \quad (48)$$

so that the integral reduces to a Beta-function, and the whole expression reads

$$\langle x^2(t) \rangle = \frac{2K_\alpha}{\Gamma(\beta)\Gamma(1-\beta)} B(\beta, \alpha - \beta + 1) t^\alpha. \quad (49)$$

Expressing the Beta-function in terms of Gamma-functions we arrive at the final result

$$\langle x^2(t) \rangle = \frac{2K_\alpha \Gamma(\alpha - \beta + 1)}{\Gamma(\alpha + 1) \Gamma(1 - \beta)} t^\alpha. \quad (50)$$

The time-dependence of MSD remains the same as for the case of free SBM, only the prefactor is altered. This result is plotted in Fig. 1 and is again in excellent agreement with simulation results (given by a green line). For $\alpha = 1$ the MSD scales linearly with time

$$\langle x^2(t) \rangle = 2K_1 (1 - \beta) t. \quad (51)$$

2. Probability density function

The PDF $p(x, t)$ for the case considered shows different behavior for small, intermediate and large values of x . Especially interesting is the case $\beta > 1 - \alpha/2$, when, for t long enough, the PDF develops a pronounced intermediate asymptotic scaling domain.

The PDF is obtained by inserting Eqs. (5), (45) and (46) into Eq. (7):

$$p(x, t) = \frac{\tau_0^{-\beta}}{\Gamma(\beta)\Gamma(1-\beta)} \frac{1}{\sqrt{4\pi K_\alpha}} \int_0^t dt' t'^{\beta-1} \left(1 + \frac{t-t'}{\tau_0}\right)^{-\beta} (t-t')^{-\alpha/2} \exp\left(-\frac{x^2}{4K_\alpha(t-t')^\alpha}\right). \quad (52)$$

To obtain the far tail of the PDF, i.e. its behavior for $|x| \gg \sqrt{4K_\alpha t^\alpha}$, we change the variable of integration to $y = (1 - t'/t)^{-\alpha}$:

$$p(x, t) = \frac{1}{\alpha\Gamma(\beta)\Gamma(1-\beta)\sqrt{4\pi K_\alpha t^\alpha}} \int_1^\infty dy y^{-\frac{1}{\alpha}-\frac{1}{2}} \left(1 - y^{-\frac{1}{\alpha}}\right)^{\beta-1} \left(\frac{\tau_0}{t} + y^{-\frac{1}{\alpha}}\right)^{-\beta} \exp\left(-\frac{x^2 y}{4K_\alpha t^\alpha}\right). \quad (53)$$

For $x^2 \gg 4K_\alpha t^\alpha$ the exponential function is decaying very fast, so that the main contribution to the integral stems from the vicinity of the lower integration bound where we take $y = 1 + \delta$ and approximate in the leading order $y^{-1/\alpha-1/2} \simeq 1$, $(1 - y^{-1/\alpha})^{\beta-1} \simeq (\delta/\alpha)^{\beta-1}$ and $(\tau_0/t + y^{-1/\alpha})^{-\beta} \simeq (1 + \tau_0/t)^{-\beta} \simeq 1$ assuming $t \gg \tau_0$. We get:

$$\begin{aligned} p(x, t) &\simeq \frac{1}{\alpha\Gamma(\beta)\Gamma(1-\beta)\sqrt{4\pi K_\alpha t^\alpha}} \exp\left(-\frac{x^2}{4K_\alpha t^\alpha}\right) \alpha^{1-\beta} \int_0^\infty d\delta \delta^{\beta-1} \exp\left(-\frac{x^2 \delta}{4K_\alpha t^\alpha}\right) \\ &= \frac{\alpha^{-\beta}}{\Gamma(1-\beta)\sqrt{4\pi K_\alpha t^\alpha}} \left(\frac{4K_\alpha t^\alpha}{x^2}\right)^\beta \exp\left(-\frac{x^2}{4K_\alpha t^\alpha}\right). \end{aligned} \quad (54)$$

Thus, the behavior of the distribution for $x^2 \gg 4K_\alpha t^\alpha$, is universally Gaussian, up to a power law correction.

Now we turn to investigation of the PDF's behavior at small and intermediate $|x|$. Changing the variable of integration to $a = 1 - t'/t$ we rewrite Eq.(52) as

$$p(x, t) = \frac{1}{\Gamma(\beta)\Gamma(1-\beta)\sqrt{4\pi K_\alpha t^\alpha}} \int_0^1 da (1-a)^{\beta-1} a^{-\alpha/2} \left(\frac{\tau_0}{t} + a\right)^{-\beta} \exp\left(-\frac{x^2}{4K_\alpha t^\alpha a^\alpha}\right), \quad (55)$$

which is the main equation to be analyzed below. The behavior of the distribution for small and intermediate x strongly depends on the relation between β and α .

Let us first consider the limit $x \rightarrow 0$. In this case the exponential in Eq.(55) tends to unity. For $t \gg \tau_0$ the term τ_0/t in the last bracket in Eq.(55) may be neglected provided the integral stays convergent under such omission, which is the case for $\beta < 1 - \alpha/2$. For $\beta > 1 - \alpha/2$ this term cannot be omitted, since it provides the necessary

regularization. As we proceed to show the two cases correspond to vastly different behavior. In the first case, omitting the corresponding term, we get

$$p(0, t) \simeq \frac{1}{\Gamma(\beta) \Gamma(1-\beta) \sqrt{4\pi K_\alpha t^\alpha}} \int_0^1 da (1-a)^{\beta-1} a^{-\alpha/2-\beta}, \quad (56)$$

so that

$$p(0, t) \simeq \frac{1}{\Gamma(\beta) \Gamma(1-\beta) \sqrt{4\pi K_\alpha t^\alpha}} B(-\alpha/2 - \beta + 1; \beta). \quad (57)$$

Expressing Beta-function in terms of Γ -functions we get an alternative form

$$p(0, t) = \frac{\Gamma(1-\beta-\alpha/2)}{\sqrt{4\pi K_\alpha t^\alpha} \Gamma(1-\alpha/2) \Gamma(1-\beta)}. \quad (58)$$

For $\alpha = 1$ we obtain, taking into account $\Gamma(1/2) = \sqrt{\pi}$,

$$p(0, t) = \frac{\Gamma(\frac{1}{2} - \beta)}{\sqrt{4\pi^2 K_1 t} \Gamma(1-\beta)} = \frac{\Gamma(1/2 - \beta) \Gamma(\beta) \sin(\pi\beta)}{\sqrt{4\pi K_1 t} \pi^{3/2}}, \quad (59)$$

where, in the last expression, Euler's reflection formula $\Gamma(1-\beta) \Gamma(\beta) = \frac{\pi}{\sin \pi\beta}$ was used. This last expression coincides with the result obtained in [22] for $\beta < 1/2$.

For $\beta > 1 - \alpha/2$ the integral Eq.(56) diverges at $x = 0$, and the term τ_0/t cannot be omitted. The expression for the PDF for $x = 0$ reads

$$p(0, t) = \frac{1}{\Gamma(\beta) \Gamma(1-\beta) \sqrt{4\pi K_\alpha t^\alpha}} \int_0^1 da (1-a)^{\beta-1} a^{-\alpha/2} (a + \tau_0/t)^{-\beta}. \quad (60)$$

The integral can be expressed via a hypergeometric function, see Eq.(2.2.6.15) of [28]:

$$\int_0^1 da (1-a)^{\beta-1} a^{-\alpha/2} (q+a)^{-\beta} = q^{-\beta} B\left(1 - \frac{\alpha}{2}, \beta\right) {}_2F_1\left(1 - \frac{\alpha}{2}, \beta, 1 - \frac{\alpha}{2} + \beta, -\frac{1}{q}\right).$$

with $q = \tau_0/t$. For $t \gg \tau_0$ the argument $z = -\frac{1}{q} = -t/\tau_0$ of the hypergeometrical function is large and tends to $-\infty$ in the course of time, so that $\arg(\beta z) = \pi$, and the asymptotic behavior of this function is given by Eq.(15.7.3) of Ref. [29]. The second term in this expansion contains the exponential $e^{\beta z}$ whose argument is negative and large, so that the whole contribution can be neglected. Therefore the final approximation in the lowest order reads:

$${}_2F_1\left(1 - \frac{\alpha}{2}, \beta, 1 - \frac{\alpha}{2} + \beta, -\frac{t}{\tau_0}\right) \simeq \frac{\Gamma(1 - \frac{\alpha}{2} + \beta)}{\Gamma(1 - \frac{\alpha}{2})} \left(\frac{\beta t}{\tau_0}\right)^{\alpha/2-1}.$$

Inserting this approximation into Eq.(60) and expressing the Beta function in terms of Gamma functions we get

$$p(0, t) \simeq \frac{\Gamma(1 - \frac{\alpha}{2} + \beta)}{\Gamma(\beta) \Gamma(1-\beta) \sqrt{4\pi K_\alpha \tau_0^\alpha}} \left(\frac{t}{\tau_0}\right)^{\beta-1}. \quad (61)$$

In both cases the PDF does not diverge for $x \rightarrow 0$.

Now let us consider intermediate values of $|x| \ll \sqrt{4K_\alpha t^\alpha}$.

For $\beta < 1 - \alpha/2$ the integral in Eq. (55) converges even in the absence of exponential term, and this term is close to unity in the most part of the integration domain except for the vicinity of the lower bound of integration. Therefore the dependence on x is weak, and the PDF at small x has a flat top where its value is given by Eq.(58). This behavior is well seen in Fig. 6, dashed curve.

For $\beta > 1 - \alpha/2$, when the integral would diverge at the lower limit if the regularizing exponential were absent, a new, interesting, intermediate regime arises. Close to this lower limit we can approximate the first bracket in the integral in Eq. (55) by unity, and change the variable of integration to $\xi = x^2/4K_\alpha t^\alpha a^\alpha$ to obtain

$$p(x, t) \simeq \frac{(4K_\alpha)^{\frac{\beta-1}{\alpha}}}{\alpha \Gamma(\beta) \Gamma(1-\beta) \sqrt{\pi}} t^{\beta-1} |x|^{-1-\frac{2\beta}{\alpha}+\frac{2}{\alpha}} \int_{\frac{x^2}{4K_\alpha t^\alpha}}^\infty \xi^{\frac{\beta-1}{\alpha}-\frac{1}{2}} e^{-\xi} d\xi, \quad (62)$$

where the integral now represents an upper incomplete Gamma function, which for the intermediate asymptotic domain $x^2 \ll 4K_\alpha t^\alpha$ can be approximated by a constant $\Gamma\left(-\frac{1+\beta}{\alpha} - \frac{1}{2}\right)$, so that

$$p(x, t) \simeq \frac{(4K_\alpha)^{\frac{\beta-1}{\alpha}} \Gamma\left(-\frac{1+\beta}{\alpha} - \frac{1}{2}\right)}{\alpha \Gamma(\beta) \Gamma(1-\beta) \sqrt{\pi}} t^{\beta-1} |x|^{-1-\frac{2\beta}{\alpha} + \frac{2}{\alpha}} \quad (63)$$

This intermediate asymptotics merges with the top of the distribution given by Eq.(61) at $|x| \sim \sqrt{4K_\alpha \tau_0^\alpha}$, and therefore stretches over the domain $\sqrt{4K_\alpha \tau_0^\alpha} \ll |x| \ll \sqrt{4K_\alpha t^\alpha}$ which at large times gets very large. Omitting all prefactors we get

$$p(x, t) \propto t^{\beta-1} |x|^{-1-\frac{2\beta}{\alpha} + \frac{2}{\alpha}} \quad (64)$$

which can be put into a scaling form $p(x, t) = t^{-\gamma} f(|x|/t^\gamma)$ with $\gamma = \alpha/2$, and $f(z) = z^{\frac{2(1-\beta)}{\alpha}-1}$.

This intermediate asymptotics is seen at long times ($t = 1000$) in two further curves depicted in Fig. 6: for $\alpha = 0.5$ and $\beta = 0.9$, where it is very narrow, and for $\alpha = 3$ and $\beta = 0.5$, where it stretches over the whole x -domain depicted. For $\alpha = 1$, $\frac{1}{2} < \beta < 1$ this expression turns to

$$p(x, t) \sim t^{\beta-1} |x|^{1-2\beta} \quad (65)$$

which is again in agreement with [22].

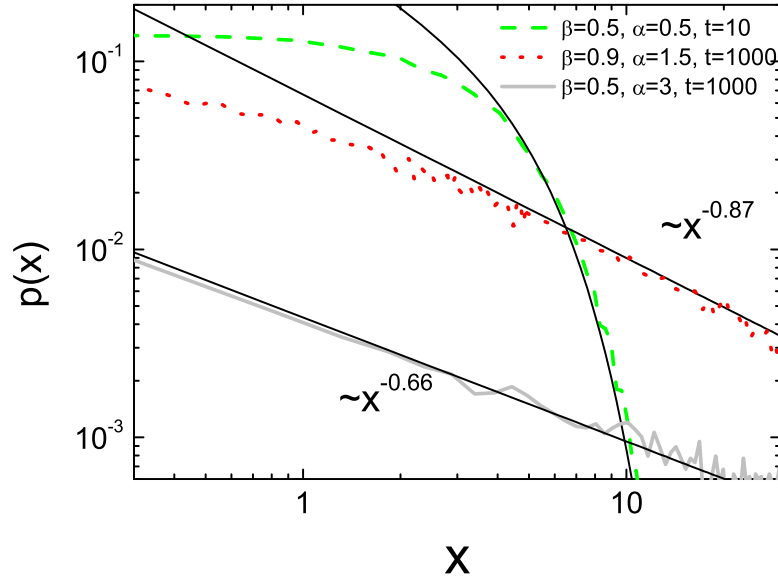


FIG. 6: PDF for SBM with power-law resetting with $0 < \beta < 1$. The dashed line (green online) corresponds to the case $\beta < 1 - \alpha/2$ and shows a flat top of the PDF crossing over to a practically Gaussian behavior, Eq.(54), at large x . Two other cases correspond to $\beta > 1 - \alpha/2$ and show the emerging intermediate asymptotic behavior, where $p(x, t) \sim t^{\beta-1} |x|^{-1-\frac{2\beta}{\alpha} + \frac{2}{\alpha}}$ according to (Eq. 64) for $\alpha = 1.5$ (red dotted line) and for $\alpha = 3$ (grey solid line). The analytical predictions for the slopes in intermediate asymptotic domains, Eq.(63), are shown with thin black straight lines.

VII. MSD AND PDF WITH POWER-LAW RESETTING, $\beta > 1$

At difference to the previous case, the rate of resetting events attains a constant value

$$\kappa(t) = \kappa = \frac{\beta - 1}{\tau_0}. \quad (66)$$

1. Mean squared displacement

Plugging Eqs. (45) and (66) into Eq. (9), we get

$$\langle x^2(t) \rangle = 2K_\alpha \tau_0^\alpha (\beta - 1) \int_0^{t/\tau_0} d\tau \tau^\alpha (1 + \tau)^{-\beta}. \quad (67)$$

The integral may be presented in terms of the hypergeometric function

$$\int_0^{t/\tau_0} d\tau \tau^\alpha (1 + \tau)^{-\beta} = \frac{(t/\tau_0)^{1+\alpha}}{1+\alpha} {}_2F_1 \left(1 + \alpha, \beta, 2 + \alpha, -\frac{t}{\tau_0} \right). \quad (68)$$

To get the power-law asymptotics of this integral we use the Pfaff transformations changing the function with the last argument equal to z into a function whose last argument is $z/(z-1)$. There are two variants of such transformations for $t/\tau_0 \rightarrow \infty$ [29]

$${}_2F_1 \left(1 + \alpha, \beta, 2 + \alpha, -\frac{t}{\tau_0} \right) = \left(1 + \frac{t}{\tau_0} \right)^{-\beta} {}_2F_1 \left(\beta, 1, 2 + \alpha, \frac{t}{t + \tau_0} \right) \quad (69)$$

$${}_2F_1 \left(1 + \alpha, \beta, 2 + \alpha, -\frac{t}{\tau_0} \right) = \left(1 + \frac{t}{\tau_0} \right)^{-1-\alpha} {}_2F_1 \left(1 + \alpha, 2 + \alpha - \beta, 2 + \alpha, \frac{t}{t + \tau_0} \right), \quad (70)$$

which, as we proceed to show, are useful in different domains of parameters. For $t \rightarrow \infty$ the last argument of the hypergeometric functions on the r.h.s. of Eqs.(69) and (70) tends to unity, and the corresponding asymptotic values of these functions can be evaluated by applying the Gauss's theorem:

$${}_2F_1(a, b, c, 1) = \frac{\Gamma(c)\Gamma(c-a-b)}{\Gamma(c-a)\Gamma(c-b)} \quad (71)$$

valid for

$$\text{Re}(c) > \text{Re}(a + b). \quad (72)$$

Using the transformation Eq.(69) and Eq. (71) we get for $\beta < \alpha + 1$:

$${}_2F_1(\beta, 1, 2 + \alpha, 1) = \frac{1 + \alpha}{1 + \alpha - \beta} \quad (73)$$

and using Eq.(70) and Eq.(71) for $\beta > \alpha + 1$ we obtain:

$${}_2F_1(1 + \alpha, 2 + \alpha - \beta, 2 + \alpha, 1) = \frac{\Gamma(2 + \alpha)\Gamma(\beta - \alpha - 1)}{\Gamma(\beta)}. \quad (74)$$

Using the corresponding asymptotic forms in Eq. (68), and substituting Eq. (68) into Eq. (67), one gets Eq. (75) below for $\beta < \alpha + 1$ and Eq. (77) for $\beta > \alpha + 1$. Thus for $\beta < \alpha + 1$ in the long time limit $t \gg \tau_0$ the MSD follows

$$\langle x^2(t) \rangle = \frac{2K_\alpha \tau_0^{\beta-1} (\beta - 1)}{\alpha - \beta + 1} t^{\alpha+1-\beta}. \quad (75)$$

The result is presented at the Fig. 1 as a grey line. The same time dependence has been observed for $1 < \beta < 2$ for non-renewal SBM [1]. In the case of ordinary Brownian motion $\alpha = 1$ and $\beta < 2$ the motion appears to be subdiffusive

$$\langle x^2(t) \rangle = 2K_1 \tau_0^{\beta-1} t^{2-\beta} \frac{\beta - 1}{2 - \beta}. \quad (76)$$

For $\beta > \alpha + 1$ the MSD stagnates:

$$\langle x^2(t) \rangle = \frac{2K_\alpha \tau_0^\alpha (\beta - 1)}{\alpha + 1} \cdot \frac{\Gamma(2 + \alpha)\Gamma(\beta - \alpha - 1)}{\Gamma(\beta)}. \quad (77)$$

This result is considerably different from the case $\beta > 2$ for non-renewal SBM, where the MSD scales according to $\sim t^{\alpha-1}$. In the case of ordinary Brownian motion, $\alpha = 1$, the MSD stagnates and attains the value

$$\langle x^2(t) \rangle = \frac{2K_1 \tau_0}{\beta - 2}. \quad (78)$$

The corresponding numerical results are presented at Fig. 1 with red ($\beta = 2.5$) and orange ($\beta = 10$) lines, respectively.

2. Probability density function

The probability density function for $\beta > 1$ may be obtained by inserting Eqs. (5), (45) and (66) into Eq. (7)

$$p(x, t) = \frac{\beta - 1}{\tau_0} \frac{1}{\sqrt{4\pi K_\alpha}} \int_0^t dt' \left(1 + \frac{t - t'}{\tau_0}\right)^{-\beta} (t - t')^{-\alpha/2} \exp\left(-\frac{x^2}{4K_\alpha(t - t')^\alpha}\right). \quad (79)$$

Changing the variable of integration to $z = \frac{x^2}{4K_\alpha(t - t')^\alpha}$ one gets

$$p(x, t) = \frac{(\beta - 1) \tau_0^{\beta-1}}{\alpha \sqrt{4\pi K_\alpha}} \left(\frac{4K_\alpha}{x^2}\right)^{\frac{\alpha/2 + \beta - 1}{\alpha}} \int_{\frac{x^2}{4K_\alpha t^\alpha}}^{\infty} dz e^{-z} z^{\frac{\beta - 1 - \alpha/2}{\alpha}}. \quad (80)$$

Performing the integration, we arrive at

$$p(x, t) = \frac{(\beta - 1) \tau_0^{\beta-1}}{\alpha \sqrt{4\pi K_\alpha}} \left(\frac{4K_\alpha}{x^2}\right)^{\frac{\alpha/2 + \beta - 1}{\alpha}} \Gamma\left(\frac{\beta - 1 + \alpha/2}{\alpha}; \frac{x^2}{4K_\alpha t^\alpha}\right). \quad (81)$$

At long times $t^\alpha \gg x^2/(4K_\alpha)$ the PDF tends to the steady state

$$p(x, t) \sim x^{-1-2\beta/\alpha+2/\alpha}. \quad (82)$$

The results of numerical simulation of PDF (Fig. 7) confirm this finding. The scaling $p(x, t) \simeq x^{-3}$ (for $\beta = 1.5$, $\alpha = 0.5$) nicely fits the obtained results at large values of x . For $\alpha = 1$ the PDF scales as $p(x, t) \sim x^{1-2\beta}$ as obtained in [22]. It is interesting to note that the PDF in its bulk tends to the steady state at long time for the whole range of $\beta > 1$, while MSD stagnates only for $\beta > 1 + \alpha$ but grows in the course of time when $1 < \beta < 1 + \alpha$, which fact stresses the absence of the overall scaling.

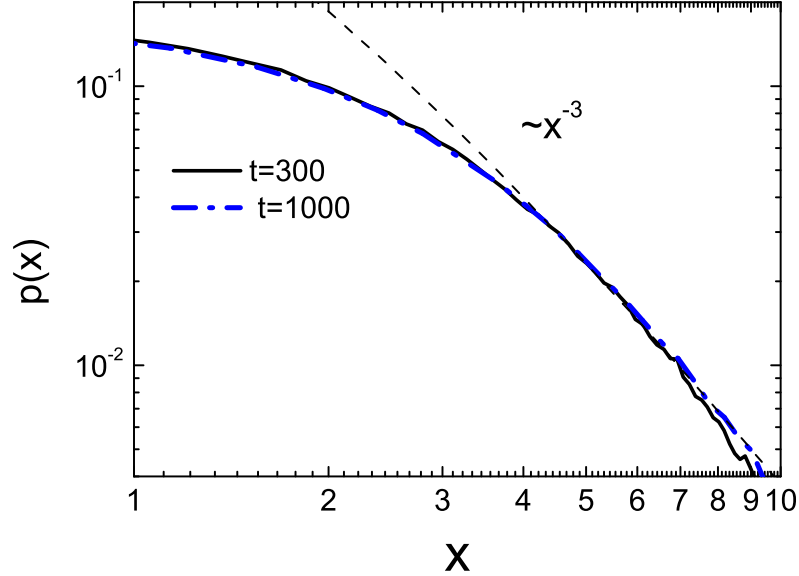


FIG. 7: PDF for SBM with power-law resetting for $t = 300$ and 1000 showing the steady state. The black dashed line corresponds to fitting with $p(x, t) \simeq x^{-3}$ (Eq. 82). Parameters: $N = 10^6$, $\alpha = 0.5$, $\beta = 1.5$.

VIII. MEAN FIRST PASSAGE TIME UNDER POWER-LAW RESETTING

The MFPT for resetting with power-law waiting time distribution can be obtained in full analogy to the case of the exponential resetting. In order to calculate the first-passage time for the power-law resetting we use Eq. (13)

with Eqs. (14) and (15), with survival probability of target, Eq. (33), the waiting time distribution between resetting events, Eq. (44), and the resetting survival probability, Eq. (45). The expression for X_0 reads:

$$X_0 = \frac{2}{\sqrt{\pi}} \int_0^\infty dt \left(1 + \frac{t}{\tau_0}\right)^{-\beta} \int_0^{\frac{x_0}{2\sqrt{K_\alpha t^\alpha}}} dae^{-a^2}. \quad (83)$$

By changing the order of integrations we arrive at the expression

$$X_0 = \frac{2}{\sqrt{\pi}} \int_0^\infty dae^{-a^2} \int_0^{\left(\frac{x_0^2}{4K_\alpha a^2}\right)^{\frac{1}{\alpha}}} \left(1 + \frac{t}{\tau_0}\right)^{-\beta} dt. \quad (84)$$

Now the inner integration may be performed explicitly to yields for the numerator in Eq. (13)

$$X_0 = \frac{2\tau_0}{\sqrt{\pi}(1-\beta)} \int_0^\infty dae^{-a^2} \left(1 + \left(\frac{A}{a^2}\right)^{\frac{1}{\alpha}}\right)^{1-\beta} - \frac{\tau_0}{1-\beta} \quad (85)$$

with

$$A = \frac{1}{\tau_0} \left(\frac{x_0^2}{4K_\alpha}\right)^{\frac{1}{\alpha}}. \quad (86)$$

On the other hand, denominator in Eq. (13) reads

$$1 - R_0 = \frac{2}{\sqrt{\pi}} \int_0^\infty dae^{-a^2} \left(1 + \left(\frac{A}{a^2}\right)^{\frac{1}{\alpha}}\right)^{-\beta}. \quad (87)$$

Changing the variables of integration in both expressions to $y = a^2$ we get

$$X_0 = \frac{\tau_0}{\sqrt{\pi}(1-\beta)} \int_0^\infty dy y^{-\frac{1}{2}} \left(1 + \left(\frac{A}{y}\right)^{\frac{1}{\alpha}}\right)^{1-\beta} e^{-y} - \frac{\tau_0}{1-\beta} \quad (88)$$

$$1 - R_0 = \frac{1}{\sqrt{\pi}} \int_0^\infty dy y^{-\frac{1}{2}} e^{-y} \left(1 + \left(\frac{A}{y}\right)^{\frac{1}{\alpha}}\right)^{-\beta} \quad (89)$$

Let us evaluate Eq. (89). The integral can be roughly estimated by splitting the integration domain into two parts (at the point A) and neglecting subleading terms:

$$\int_0^\infty dy y^{-\frac{1}{2}} e^{-y} \left(1 + Ay^{-\frac{1}{\alpha}}\right)^{-\beta} \simeq \int_0^A dy e^{-y} A^{-\beta} y^{\frac{\beta}{\alpha} - \frac{1}{2}} + \int_A^\infty dy y^{-\frac{1}{2}} e^{-y}. \quad (90)$$

In the first integral we have neglected unity compared to $Ay^{-\frac{1}{\alpha}}$ and in the second one we neglect $Ay^{-\frac{1}{\alpha}}$ compared to 1. Both integrals are now incomplete Gamma functions. X_0 can be calculated analogously. The final result reads

$$\tau \simeq \frac{\tau_0}{\beta - 1} \times \frac{\sqrt{\pi} \operatorname{erf}(\sqrt{A}) - A^{1-\beta} \gamma\left(A, \frac{\beta-1}{\alpha} + \frac{1}{2}\right)}{A^{-\beta} \gamma\left(A, \frac{\beta}{\alpha} + \frac{1}{2}\right) + \sqrt{\pi} \operatorname{erfc}(\sqrt{A})}. \quad (91)$$

For $A = \frac{1}{\tau_0} \left(\frac{x_0^2}{4K_\alpha}\right)^{\frac{1}{\alpha}} \rightarrow \infty$ corresponding to the target located far from origin the MFPT tends to

$$\tau = \frac{\sqrt{\pi} \tau_0^{1-\beta}}{(\beta - 1) \Gamma\left(\frac{\beta}{\alpha} + \frac{1}{2}\right)} \left(\frac{x_0^2}{4K_\alpha}\right)^{\frac{\beta}{\alpha}}. \quad (92)$$

The results of numerical simulations together with the predictions of Eq. (91) are shown in Fig. 8. One can see that for distant targets ($x_0 = 10$) the search becomes more efficient in the case of superdiffusion in a large domain of β .

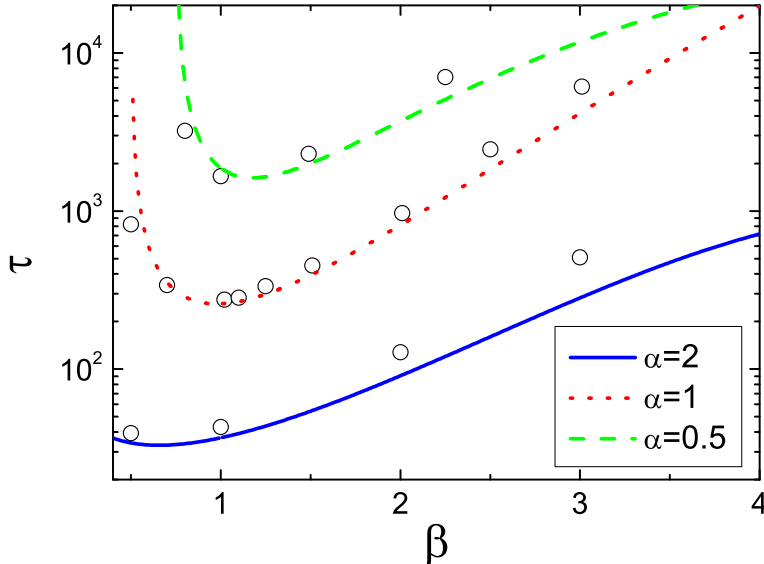


FIG. 8: Mean FPT as function of β for $x_0 = 10$. The results of numerical simulation are depicted by circles. The analytical results, Eq. (91), are given by lines.

IX. CONCLUSIONS

In the present work we study analytically and numerically the properties of scaled Brownian motion with time-dependent diffusion coefficient $D(t) \sim t^{\alpha-1}$ interrupted by random resetting to the origin. The resetting process is a renewal one with either exponential or power law distribution of waiting times between the resetting events. At difference to our previous work, diffusion coefficient is also reset, so that the whole process is now a renewal one. This memory erasing significantly changes the properties of the process compared to the one discussed in [1]. The main results here are as follows: For exponential resetting and power-law resetting with $\beta > 1 + \alpha$ the mean-squared displacement (MSD) at long times stagnates. For $\beta < 1$ the time dependence of the MSD remains the same as in the case of free scaled Brownian motion, albeit with a different prefactor. In the intermediate domain $1 < \beta < 1 + \alpha$ we revealed $\langle x^2 \rangle \sim t^{1+\alpha-\beta}$, so the behavior of the MSD is defined by the interplay of the parameters α and β .

In the case of the exponential resetting the probability distribution function (PDF) tends to the steady state with stretched or squeezed exponential tail $p(x, t) \simeq \exp\left(-\gamma|x|^{\frac{2}{\alpha+1}}\right)$. For the power-law resetting with $\beta > 1$ it also attains a time-independent form, now $p(x, t) \sim x^{-1-\frac{2\beta}{\alpha}+\frac{2}{\alpha}}$. It is interesting to note that for $\beta > 1 + \alpha$ both MSD and PDF tend to the stationary state while for $1 < \beta < 1 + \alpha$ only the PDF in the bulk is stationary but MSD grows continuously with time. For $\beta < 1$ the behavior of the PDF depends on the relation between the exponents β and α . For $\beta > 1 - \alpha/2$ x -dependence of the PDF for $\sqrt{4K_\alpha\tau_0^\alpha} \ll |x| \ll \sqrt{4K_\alpha t^\alpha}$ is the same as in the previous case, but now the time-dependence also appears: $p(x, t) \sim t^{\beta-1}|x|^{-1-\frac{2\beta}{\alpha}+\frac{2}{\alpha}}$. For long times this intermediate domain covers practically the whole bulk of the distribution. For $\beta < 1 - \alpha/2$ the PDF in the center of the distribution is flat, with a Gaussian tail at $x \gg \sqrt{4K_\alpha t^\alpha}$.

Below we present the MSD and PDF in the form of the table.

TABLE I: MSD and PDF for the renewal power-law resetting

	$0 < \beta < 1 - \alpha/2$	$1 - \alpha/2 < \beta < 1$	$1 < \beta < 1 + \alpha$	$\beta > 1 + \alpha$
MSD	$\sim t^\alpha$	$\sim t^\alpha$	$\sim t^{\alpha+1-\beta}$	stagnates
PDF	flat top, Gaussian tail	$\sim t^{\beta-1} x ^{-1-2\beta/\alpha+2/\alpha}$	$\sim x ^{-1-2\beta/\alpha+2/\alpha}$	$\sim x ^{-1-2\beta/\alpha+2/\alpha}$

For comparison we also provide here the results for the non-renewal case [1]:

TABLE II: MSD and PDF for the non-renewal power-law resetting

	$0 < \beta < 1/2$	$1/2 < \beta < 1$	$1 < \beta < 2$	$\beta > 2$
MSD	$\sim t^\alpha$	$\sim t^\alpha$	$\sim t^{\alpha+1-\beta}$	$\sim t^{\alpha-1}$
PDF	no universal scaling, Gaussian tail	$\sim x ^{1-2\beta} t^{\alpha(\beta-1)}$	$\sim x ^{1-2\beta} t^{(1-\beta)(1-\alpha)}$	$\sim x ^{1-2\beta} t^{(1-\beta)(1-\alpha)}$

The overall renewal nature of the whole process allowed us also to calculate the mean first passage time to a target. This MFPT is investigated as a function of parameters of the model for the corresponding cases of Poissonian and power-law resetting.

X. ACKNOWLEDGEMENTS

A.S.B. thanks Carlos Mejiá-Monasterio, Arnab Pal and Shlomi Reuveni for fruitful discussions. AVC acknowledges the financial support by the Deutsche Forschungsgemeinschaft within the project ME1535/6-1.

-
- [1] A.S. Bodrova, A.V. Chechkin, I.M. Sokolov, submitted (2018).
 - [2] A.V. Chechkin, I.M. Sokolov, Phys. Rev. Lett. **121**, 050601 (2018).
 - [3] O. Benichou, C. Loverdo, M. Moreau, and R. Voituriez, Rev. Mod. Phys. **83**, 81 (2011)
 - [4] A. Montanari and R. Zecchina, Phys. Rev. Lett. **88**, 178701 (2002).
 - [5] S. Reuveni, M. Urbach, and J. Klafter, Proc. Natl. Akad. Sci. U.S.A. **111**, 4391 (2014).
 - [6] É. Roldán, A. Lisica, D. Sánchez-Taltavull, and S.W. Grill, Stochastic resetting in backtrack recovery by RNA polymerases, Phys. Rev. E **93**, 062411 (2016).
 - [7] S. Redner, A Guide to First-Passage processes. Cambridge University Press, Cambridge, UK (2007).
 - [8] R. Metzler, G. Oshanin and S. Redner, eds., First Passage Phenomena and Their Applications. World Scientific, Singapore (2014).
 - [9] M. R. Evans and S. N. Majumdar, Phys. Rev. Lett. **106**, 160601 (2011).
 - [10] M. R. Evans and S. N. Majumdar, J. Phys. A: Math. Theor. **44**, 435001 (2011).
 - [11] M.R. Evans, S.N. Majumdar and K. Mallick. J. Phys. A: Math. Theor. **46**, 185001 (2013).
 - [12] M.R. Evans and S.N. Majumdar. J. Phys. A: Math. Theor. **47**, 285001 (2014).
 - [13] U. Bhat, C. de Bacco, S. Redner. J. Stat Mech. 083401 (2016).
 - [14] A. Scacchi, A. Sharma. Mol. Phys. **116**, 460 (2018).
 - [15] E. Gelenbe, Phys. Rev. E **82**, 061112 (2010).
 - [16] L. Kuśmierz, S. N. Majumdar, S. Sabhapandit, and G. Schehr, Phys. Rev. Lett. **113**, 220602 (2014).
 - [17] L. Kuśmierz, E. Gudowska-Nowak. Phys. Rev. E **92**, 052127 (2015).
 - [18] A. Pal, A. Kundu and M. R. Evans, J. Phys. A: Math. Theor. **49**, 225001 (2016).
 - [19] S. Eule and J. J. Metzger, New J. Phys. **18**, 033006 (2016).
 - [20] S. Reuveni. Phys. Rev. Lett. **116**, 170601 (2016).
 - [21] A. Pal and S. Reuveni, Phys. Rev. Lett. **118**, 030603 (2017).
 - [22] A. Nagar and S. Gupta. Phys. Rev. E **93**, 060102 (2016).
 - [23] S. C. Lim and S. V. Muniandy, Phys. Rev. E **66**, 021114 (2002).
 - [24] J.-H. Jeon, A. V. Chechkin, and R. Metzler, Phys. Chem. Chem. Phys. **16**, 15811 (2014).
 - [25] F. Thiel and I. M. Sokolov, Phys. Rev. E **89**, 012115 (2014).
 - [26] S.N. Majumdar, S. Sabhapandit, and G. Schehr, PRE **91**, 052131 (2015).
 - [27] V.V. Palyulin, A.V. Chechkin, and R. Metzler, PNAS **111**, 2931-2936 (2014).
 - [28] A.P.Prudnikov, Yu.A.Brychov and O.I.Marichev, Integrals and Series, Gordon & Breach, New York, 1986.
 - [29] M. Abramowitz and I. A. Stegun. Handbook of Mathematical Functions. Dover, Publications, New York, 1965.